Propagators of resonances and rescatterings of the decay products

A.V. Anisovich[+], V.V. Anisovich[+], M.A. Matveev[+], Nyiri[*],
A.V. Sarantsev[+], A.N. Semenova[+],

September 14, 2021

[+]*National Research Centre "Kurchatov Institute": Petersburg Nuclear Physics Institute, Gatchina, 188300, Russia*

[*]*Institute for Particle and Nuclear Physics, Wigner RCP, Budapest 1121, Hungary*

Abstract

Hadronic resonance propagators which take into account the analytical properties of decay processes are built in terms of the dispersion relation technique. Such propagators can describe multi-component systems, for example, those when quark degrees of freedom create a resonance state, and decay products correct the corresponding pole by adding hadronic deuteron-like components. Meson and baryon states are considered, examples of particles with different spins are presented.

1   Introduction

Nowadays we face a pressing request for studying multi-component systems, in particular, those with concurrent parts of quark and hadron degrees of freedom. Recent experimental evidences for exotic states (see Refs. [1–3] and references therein) definitely indicate the important role of both short-distance physics (predominantly quark-gluon one) and long-distance hadron physics where the notion of deuteron-like systems or molecules looks quite appropriate.[4,5] The active discussion of the pentaquark topic is in line with this trend.[6–16]

The two-component structure of resonances can reveal itself in propagators of the resonances. A corresponding consideration of meson resonances is performed in Ref. [17] for tetraquark systems with hidden charm where meson states for decay processes were taken into account (but with non-relativistic spin wave functions). In this paper we present the relativistic consideration of both meson and baryon systems with spins. An important point in this consideration is to keep the analytic amplitude with correct singular structure.
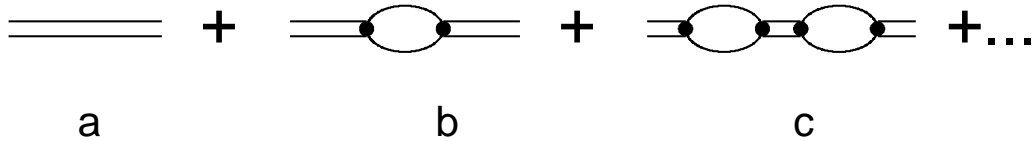
Figure 1: Graphic representation of the Breit-Wigner pole term as an infinite set of transitions *resonance state → decay products → resonance state.*

Let us turn to a standard description of resonances. The Breit-Wigner pole[18] gives us a description of a resonance state in a form of particle propagator, for non-relativistic and relativistic cases the pole amplitudes read:

$$\text{non} - \text{relativistic}: \qquad \frac{G_i G_j}{E_0 - E - i\frac{\Gamma}{2}}, \qquad (1)$$

$$\text{relativistic}: \qquad \frac{G_i G_j}{M^2 - s - i\Gamma M}.$$

Here E is the energy of the non-relativistic system, and E_0 is the energy of the resonance level; Γ is the width of the resonance and G_i, G_j are couplings with initial and final states. For the relativistic case the total energy $\sqrt{s}$ includes the mass of the system and M refers to the resonance mass.

The energy independent width corresponds to a rough approximation, for the study of the πp scattering in the $\Delta(1240)$ region (hadrons πp are in the P-wave) Gell-Mann and Watson[19] suggested to use the energy dependent width:

$$\Gamma \to \gamma \frac{k_{\pi p}^3}{1 + R^2 k_{\pi p}^2}, \qquad (2)$$

where $k_{\pi p}$ is the relative momentum of πp in the c.m. system. Actually the width in the form Eq. (2) takes into account the threshold singularity (k^{2L+1} where $L = 1$ is the orbital momentum) inherent to transitions $\Delta \to \pi p \to \Delta$. The threshold singularity appears when we consider a set of diagrams related to decay processes such as shown in Fig. 1. But Eq. (2) contains also singularities which are absent in the scattering amplitude.

First, there are those related to

$$k_{\pi p} = \sqrt{\frac{[s - (m_p + m_\pi)^2][s - (m_p - m_\pi)^2]}{4s}}, \qquad (3)$$

namely, the square root singularities at $s = 0$ and $s = (m_p - m_\pi)^2$; the form factor $1/[1 + R^2 k_{\pi p}^2]$ has a pole singularity which gives zeros in the related amplitudes. For the precise use of amplitudes with the resonance propagators one needs to take into account the contributions of decay processes without false singularities, i.e. to use the corresponding loop diagrams.

The paper is assembled as follows. In Section 2 spinless hadron resonances are given and multi-channel cases are considered. Sections 3 and 4 are devoted to particles with spins, correspondingly, to meson and baryon resonances. In Section 5 we investigate the problem of

2

formation of the deuteron-like components in states belonging originally to quark-gluon ones. In Appendices A, B, C elements of technique for working with loop diagrams of spin particles are given.

2 Propagators for meson resonances

For the inclusion of the loop diagrams into the resonance propagator the D-function technique is appropriate, we use it here. First, we consider scalar mesons, after that we generalize the consideration to cases of spin particles.

2.1 Loop diagrams in the resonance propagator

The set of diagrams of Fig. 1 reads:

$$\frac{1}{-s+m^2} + \frac{1}{-s+m^2}B(s)\frac{1}{-s+m^2} + \frac{1}{-s+m^2}B(s)\frac{1}{-s+m^2}B(s)\frac{1}{-s+m^2} + ...$$
$$= \frac{1}{-s+m^2-B(s)}, \tag{4}$$

where $B(s)$ is the contribution of the loop diagram related to the resonance decay (in Fig. 1 it is supposed that we deal with a two-particle decay). If a resonance state decays into several channels, one should replace:

$$B(s) \to \sum_{\ell=1}^{n} B^{(\ell)}(s) \tag{5}$$

where n is the number of open channels. In the standard Breit$-$Wigner approach the s-independent loop diagrams are used:

$$M^2 = m^2 - \sum_{\ell=1}^{n} ReB^{(\ell)}(M^2), \quad M\Gamma = \sum_{\ell=1}^{n} ImB^{(\ell)}(M^2). \tag{6}$$

Following the Gell-Mann$-$Watson prescription[19] one takes into account the s-dependent imaginary part of the loop diagrams:

$$ImB^{(\ell)}(s) = \rho_\ell(s)g_\ell^2(s), \quad \rho_\ell(s) = \frac{k_\ell^{2L_\ell+1}}{8\pi\sqrt{s}}, \tag{7}$$

where $\rho_\ell(s)$ is the phase space for loop-diagram particles, $g_\ell(s)$ is the vertex for the transition *resonance state$\to$decay particles of the ℓ-state*, and L_ℓ is the orbital momentum of particles in the loop diagram. But, as it was discussed above, the imaginary part alone contains false singularities. For reproducing the analytical amplitude correctly, one needs to take into account the real part of $B^{(\ell)}(s)$ as well.

2.2 D-function and loop diagrams with $L = 0$ for the one-pole amplitude

Let us consider a loop diagram above the threshold, at $s > (M_a + M_b)^2$. The equation for one-pole and one-channel D-function reads:

$$D = d + D B d, \quad d = \frac{1}{m^2 - s}, \quad B = \int\limits_{(M_a+M_b)^2}^{\infty} \frac{ds'}{\pi} \frac{G^2 \rho(s')}{s' - s - i0}. \tag{8}$$

Here m is a bare mass of this state, the factor B goes from the loop diagram formed by hadrons (a, b), and M_a, M_b are masses of the loop mesons. The phase space factor for the S-wave state $(L = 0)$ is:

$$\rho(s) = \frac{\sqrt{[s-(M_a+M_b)^2][s-(M_a-M_b)^2]}}{16\pi s}. \tag{9}$$

The convergency of the integral for $B(s)$ can be organized either due to introducing a s-dependence of the vertex $G \to G(s')$ or by switching the subtraction procedure:

$$B(s) = \int\limits_{(M_a+M_b)^2}^{\infty} \frac{ds'}{\pi} \cdot \frac{G^2 \rho(s')}{s' - s - i0} \rightarrow$$

$$b_0 + \int\limits_{(M_a+M_b)^2}^{\infty} \frac{ds'}{\pi} \frac{[s-(M_a+M_b)^2] \cdot G^2 \rho(s')}{(s'-(M_a+M_b)^2)(s'-s-i0)}. \tag{10}$$

Imposing $G^2 = 1$ we write for positive s, $s > (M_a + M_b)^2$:

$$
\begin{aligned}
B(s) &= b_0 + \beta \frac{(M_a + M_b)^2 - s}{s(M_a + M_b)^2} + \frac{\sqrt{[s - (M_a + M_b)^2][s - (M_a - M_b)^2]}}{16\pi s} \times \\
&\qquad \left[\frac{1}{\pi} \ln \frac{\sqrt{s - (M_a - M_b)^2} - \sqrt{s - (M_a + M_b)^2}}{\sqrt{s - (M_a - M_b)^2} + \sqrt{s - (M_a + M_b)^2}} + i \right], \\
\beta &= -\frac{M_a^2 - M_b^2}{16\pi^2} \ln \frac{M_a}{M_b}.
\end{aligned}
\tag{11}
$$

The point $s = (M_a + M_b)^2$ is singular. For $s < (M_a + M_b)^2$ we write $\sqrt{s - (M_a + M_b)^2} \to i\sqrt{(M_a + M_b)^2 - s}$, the points $s = (M_a - M_b)^2$ and $s = 0$ are not singular, the pole singularity at $s = 0$ is cancelled due to the term with β.

The subtraction constant b_0 regulates a value of the meson component near the threshold, i.e. the fraction of the deuteron-like system. The zero value of the deuteron-like fraction is realized with $B(s)\big|_{s=(M_a+M_b)^2} = 0$, namely at: $b_0 = 0$.

We have eliminated the pole singularity in the loop diagram introducing the cancellation term $\frac{\beta}{s}$. Let us remark, however, that the pole singularity in the loop diagram does not violate the analytical structure of the total amplitude because the poles in the loop diagram do not lead to new singularities but to zeros of the amplitude (see Appendix A).

2.3 One-pole propagator with non-zero orbital momenta of mesons, $L \neq 0$

The loop diagram expression of Eq. (11) gives a possibility to write down analogous terms with non-zero orbital momenta, $L_\ell \neq 0$, and taking into account form factor $G_\ell(s)$:

$$B_\ell^{L_\ell}(s) = k_\ell^{2L_\ell} G_\ell(s) B_\ell(s) G_\ell(s) \,. \tag{12}$$

Factor $G_\ell(s)$ is to be chosen in a form without the violation of the analytical structure of the amplitude, for example, one can use the simple exponential form $G_\ell(s) = G_0 \exp(-R_\ell^2 s)$. The exponential form guarantees the convergence of the loop diagrams. One can use the inverse polynomial function as well: $G_\ell(s) \sim 1/P_n(s)$ with $P_n(s) = \sum_{\nu=0}^{n} a_\nu s^\nu$ because zeros of the $P_n(s)$ are not singular points of the amplitude.

2.4 Two-pole amplitude

The two-pole D-matrix functions can be written as solutions of the following equations:

$$
\begin{aligned}
D_{11} &= d_1 + D_{11} B_{11} d_1 + D_{12} B_{21} d_1 \,, \\
D_{12} &= D_{11} B_{12} d_2 + D_{12} B_{22} d_2 \,, \\
D_{21} &= D_{22} B_{21} d_1 + D_{21} B_{11} d_1 \,, \\
D_{22} &= d_2 + D_{22} B_{22} d_2 + D_{21} B_{12} d_2 \,,
\end{aligned}
\tag{13}
$$

that results in the explicit form

$$D_{12} = \frac{d_1 B_{12} d_2}{(1 - B_{22} d_2)(1 - B_{11} d_1) - d_1 B_{12} d_2 B_{21}} \,, \tag{14}$$

$$D_{11} = \frac{d_1 (1 - B_{22} d_2)}{(1 - B_{22} d_2)(1 - B_{11} d_1) - d_1 B_{12} d_2 B_{21}} \,.$$

Here $B_{if} = B_{fi}$, zeros of the denominator determine positions of the poles. Expressions for D_{12} and D_{22} are given by the replacement of indices $1 \rightleftharpoons 2$. We have $D_{12} = D_{21}$ and a common denominator for all D-functions.

If B_{12} is small we have two separate poles in the region of studies similar to that discussed in the one-pole case. Non-zero B_{12} means a mixture of the input pole states and the change of their masses and widths. At large B_{if} additional poles can appear, the additional poles mean the appearance of new two-meson states created by mesons of the loop diagrams.

2.5 D-matrix with an arbitrary number of poles

The equation for the D-matrix can be written as follows:

$$\hat{D}(s) = \hat{d}(s) + \hat{D}(s) \hat{B}(s) \hat{d}(s), \tag{15}$$

that gives:

$$\hat{D}(s) = \hat{d}(s) \frac{1}{I - \hat{B}(s) \hat{d}(s)} \tag{16}$$

where

$$\hat{D}(s) = \begin{vmatrix} D_{11}(s) & D_{12}(s) & D_{13}(s) & \cdot & \cdot \\ D_{21}(s) & D_{22}(s) & D_{23}(s) & \cdot & \cdot \\ D_{31}(s) & D_{32}(s) & D_{33}(s) & \cdot & \cdot \\ \cdot & \cdot & \cdot & \cdot & \cdot \\ \cdot & \cdot & \cdot & \cdot & \cdot \end{vmatrix}, \quad \hat{d}(s) = \begin{vmatrix} d_1(s) & 0 & 0 & \cdot & \cdot \\ 0 & d_2(s) & 0 & \cdot & \cdot \\ 0 & 0 & d_3(s) & \cdot & \cdot \\ \cdot & \cdot & \cdot & \cdot & \cdot \\ \cdot & \cdot & \cdot & \cdot & \cdot \end{vmatrix},$$

$$\hat{B}(s) = \begin{vmatrix} B_{11}(s) & B_{12}(s) & B_{13}(s) & \cdot & \cdot \\ B_{21}(s) & B_{22}(s) & B_{23}(s) & \cdot & \cdot \\ B_{31}(s) & B_{32}(s) & B_{33}(s) & \cdot & \cdot \\ \cdot & \cdot & \cdot & \cdot & \cdot \\ \cdot & \cdot & \cdot & & \cdot \end{vmatrix}. \tag{17}$$

and

$$d_i(s) = \frac{1}{m_i^2 - s}, \tag{18}$$

$$B_{if}(s) = \sum_\ell k_\ell^{2L_\ell} G_{i\ell}(s) B_\ell(s) G_{\ell f}(s).$$

Recall that for the one-pole case $B_\ell(s) \equiv B_{\{ab\}}(s) \equiv B(s)$ is given by Eq. (11).

3 D-function for mesons with spin

We consider here meson resonances with spin. First, as elucidation examples, cases with scalar (S), pseudoscalar (P), vector (V), and tensor (T) particles are considered, after that the D-functions for particles with higher spins are presented.

3.1   Transition $1^- \rightarrow [1^-(k_a) + 0^+(k_b)]_{S-wave} \rightarrow 1^-$

To calculate the propagator we should calculate the imaginary part of the loop diagram and restore the real part using Eq. (11). In this procedure the S-wave terms for the transitions $V^{(in)} \rightarrow [V^{(a)} + S^{(b)}]_{S-wave} \rightarrow V^{(fin)}$ (see Fig. 1) are written as follows:

$$\frac{g_{\alpha\beta}^{\perp P}}{m^2 - s} + \frac{g_{\alpha\alpha'}^{\perp P}}{m^2 - s} G_{(ab)}(s) \int \frac{d^4k_1 d^4k_2}{i(2\pi)^4}$$

$$\times \frac{\delta(P - k_a - k_b) g_{\alpha'\beta'}^{\perp k_a}}{(M_a^2 - k_a^2 - i0)(M_b^2 - k_2^b - i0)} G_{(ab)}(s) \cdot \frac{g_{\beta'\beta}^{\perp P}}{m^2 - s} + \dots$$

$$= \frac{g_{\alpha\beta}^{\perp P}}{m^2 - s} \left[1 + \frac{G_{(ab)}(s) S_V^{VS}(s) B(s) G_{(ab)}(s)}{m^2 - s} + \dots \right]$$

$$= \frac{g_{\alpha\beta}^{\perp P}}{m^2 - s - G_{(ab)}(s) S_V^{VS}(s) B(s) G_{(ab)}(s)}. \tag{19}$$

Here $g_{\alpha\beta}^{\perp P} = g_{\alpha\beta} - \frac{P_\alpha P_\beta}{P^2}$ and

$$3 S_V^{VS}(s) = g_{\alpha\alpha'}^{\perp P} g_{\alpha'\beta'}^{\perp k_a} g_{\beta'\alpha}^{\perp P} = [2 + \frac{(k_a P)^2}{s M_a^2}], \tag{20}$$

with vectors k_1, k_2 being the mass-on-shell values ($k_a^2 = M_a^2$, $k_b^2 = M_b^2$) that result:

$$2(k_a P) = s + M_a^2 - M_b^2. \tag{21}$$

The width is determined by the imaginary part of the loop diagram, and $S_V^{VS}(s)$ is a meromorphic function.

3.2 Transition $1^- \to [1^-(k_a) + 0^-(k_b)]_{P-wave} \to 1^-$

For the propagator $V^{(in)} \to [V^{(a)} + \pi^{(b)}]_{P-wave} \to V^{(fin)}$ we write:

$$\frac{g_{\alpha\beta}^{\perp P}}{m^2 - s} \quad + \quad \frac{g_{\alpha\alpha'}^{\perp P}}{m^2 - s} G_{(ab)}(s) \int \frac{d^4 k_a}{i(2\pi)^4}$$

$$\times \quad \frac{\epsilon_{\alpha'\gamma' k_a P} \, g_{\gamma'\delta'}^{\perp k_a} \, \epsilon_{\delta'\beta' P k_a}}{(M_a^2 - k_a^2 - i0)(M_b^2 - k_b^2 - i0)} G_{(ab)}(s) \frac{g_{\beta'\beta}^{\perp P}}{m^2 - s} + ...$$

$$= \quad \frac{g_{\alpha\beta}^{\perp P}}{m^2 - s}\Big[1 + \frac{G_{(ab)}(s) S_V^{V\pi}(s) B(s) G_{(ab)}(s)}{m^2 - s} + ...\Big]$$

$$= \quad \frac{g_{\alpha\beta}^{\perp P}}{m^2 - s - G_{(ab)}(s) S_V^{V\pi}(s) B(s) G_{(ab)}(s)}, \tag{22}$$

with spin factor $S_V^{V\pi}(s)$ determined by mass-on-shell mesons, $k_a^2 = M_a^2$, $k_b^2 = M_b^2$:

$$3\, S_V^{V\pi}(s) = g_{\alpha\alpha'}^{\perp P}\epsilon_{\alpha'\gamma' k_a P} \, g_{\gamma'\delta'}^{\perp k_a} \, \epsilon_{\delta'\beta' P k_a} g_{\beta'\alpha}^{\perp P} = \frac{2s}{M_a M_b}\Big[\frac{(k_a P)^2}{s} - M_a^2\Big]. \tag{23}$$

Recall that the loop diagram factor $B(s)$ is given in Eq. (11).

3.3 The S-wave transition of vector-axial state
$1^+ \to [1^-(k_a) + 1^-(k_b)]_{S-wave} \to 1^+$

For the transition $A^{(in)} \to [V^{(a)} + V^{(b)}]_{S-wave} \to A^{(fin)}$ the second diagram of the set of Fig. 1 reads:

$$\frac{g_{\alpha\alpha'}^{\perp P}}{m^2 - s} i\epsilon_{\alpha'\gamma\gamma'' P} \cdot G_{(ab)}(s) \int \frac{d^4 k_a d^4 k_b}{i(2\pi)^4}\delta(P - k_a - k_b) \tag{24}$$

$$\times \frac{g_{\gamma'\delta'}^{\perp k_a} g_{\gamma''\delta''}^{\perp k_b}}{(M_a^2 - k_a^2 - i0)(M_b^2 - k_b^2 - i0)} G_{(ab)}(s) \cdot (-i)\epsilon_{\delta'\delta''\beta' P} \frac{g_{\beta'\beta}^{\perp P}}{m^2 - s}$$

with the notation $\epsilon_{\delta'\delta''\beta' P} = \epsilon_{\delta'\delta''\beta'\beta''} P_{\beta''}$ and $g_{\alpha\beta}^{\perp P} = g_{\alpha\beta} - \frac{P_\alpha P_\beta}{P^2}$.

The spin factor of the second term is equal to:

$$g_{\alpha\alpha'}^{\perp P}\epsilon_{\alpha'\gamma\gamma'' P} \cdot g_{\gamma'\delta'}^{\perp k_a} g_{\gamma''\delta''}^{\perp k_b} \cdot \epsilon_{\delta'\delta''\beta' P} \cdot g_{\beta'\beta}^{\perp P} = g_{\alpha\beta}^{\perp P} S_A^{V_a V_b}(s). \tag{25}$$

Let us remind that here we mean $M_a^2 = k_a^2$ an $M_b^2 = k_b^2$. The resonance propagator is written as follows:

$$J = 1: \quad \frac{g_{\alpha\beta}^{\perp P}}{m^2 - s - G_{(ab)}(s) S_A^{V^{(a)} V^{(b)}}(s) B(s) G_{(ab)}(s)}. \tag{26}$$

3.4 The S-wave transitions $S \to V^{(a)} + V^{(b)} \to S$, and $T \to V^{(a)} + V^{(b)} \to T$

The propagator for resonance with $J = 0$ is:

$$J = 0 : \qquad \frac{1}{m^2 - s - G_{(ab)}(s)S_S^{V^{(a)}V^{(b)}}(s)B(s)G_{(ab)}(s)}, \qquad (27)$$

$$S_S^{V^{(a)}V^{(b)}}(s) = \frac{1}{3}G^2(s)\Gamma_0^{\gamma'\gamma''}(\perp P) \cdot O_{\gamma'}^{\delta'}(\perp k_a)O_{\delta''}^{\gamma''}(\perp k_b) \cdot \Gamma_0^{\delta'\delta''}(\perp P),$$

$$\Gamma_0^{\delta'\delta''}(\perp P) = O_{\delta'}^{\delta''}(\perp P).$$

Here we introduce the vertex function $\Gamma_0^{\gamma'\gamma''}(\perp P)$ and denote $O_{\gamma''}^{\gamma'}(\perp P) = g_{\gamma''\gamma'}^{\perp P}$, see Appendix B for details.

We write for $J = 2$:

$$J = 2 : \qquad \frac{O_{\beta_1\beta_2}^{\alpha_1\alpha_2}(\perp P)}{m^2 - s - G^{(ab)}(s)S_T^{V^{(a)}V^{(b)}}(s)B(s)G^{(ab)}(s)}, \qquad (28)$$

$$S_2(s, k_1^2, k_2^2) = \frac{1}{5}G^2(s)O_{\alpha_1\alpha_2}^{\gamma'\gamma''}(\perp P) \cdot O_{\gamma'}^{\delta'}(\perp k_1)O_{\gamma''}^{\delta''}(\perp k_2) \cdot O_{\delta'\delta''}^{\alpha_1\alpha_2}(\perp P).$$

The operator for the tensor state, $O_{\alpha_1\alpha_2}^{\gamma'\gamma''}(\perp P)$, is given in Appendix B.

4 Baryon resonances

Propagators for baryon resonances can be constructed in a way analogous to that for mesons but with some complication, namely: determining one-channel rescattering we face two basic loop functions, $B(s)$ and $\widetilde{B}(s)$.

First, we present several examples of propagators for spin-$1/2$ resonances. Then the cases with larger spins ($J > 1/2$) are discussed. The technique used here for fermions with spins $J > 1/2$ is given in Appendix C.

4.1 Spin-$1/2$ state and its decay with the emission of a scalar meson

We consider here transitions of the type $N^*(\frac{1}{2}^+) \to [S(0^+) + N(\frac{1}{2}^+)] \to N^*(\frac{1}{2}^+)$.

The first two terms of the series shown in Fig. 1 are written as:

$$\frac{\hat{P} + \sqrt{s}}{m^2 - s} + \frac{\hat{P} + \sqrt{s}}{m^2 - s} \cdot G(s) \, B_{N^*}(s) \, G(s) \cdot \frac{\hat{P} + \sqrt{s}}{m^2 - s}, \qquad (29)$$

where the loop function $B_{N^*}^{SN}(s) = B_{N^*}(s) \cdot 2\sqrt{s}$ has the following form:

$$B_{N^*}^{SN}(s) \quad = \int \frac{d^4k}{i(2\pi)^4} \frac{\hat{k} + M_N}{(k^2 - M_N^2 - i0)((P - k)^2 - M_S^2 - i0)} \cdot (\hat{P} + \sqrt{s})$$

$$= \int \frac{d^4k}{i(2\pi)^4} \quad \frac{\frac{(kP)}{P^2}\hat{P} + M_N}{(k^2 - M_N^2 - i0)((P-k)^2 - M_S^2 - i0)} \cdot (\hat{P} + \sqrt{s})$$

$$= \int \frac{d^4k}{i(2\pi)^4} \quad \frac{\frac{(kP)}{s}\sqrt{s} + M_N}{(k^2 - M_N^2 - i0)((P-k)^2 - M_S^2 - i0)} \cdot 2\sqrt{s} \,. \tag{30}$$

We use $k = k^{\perp} + \frac{(kP)}{P^2}P$ and $(\hat{P} + \sqrt{s})(A\hat{P} + B)(\hat{P} + \sqrt{s}) = (\hat{P} + \sqrt{s})(A\sqrt{s} + B) \cdot 2\sqrt{s}$; recall that the loop diagram hadrons are mass-on-shell in the imaginary part, and $2(kP) = s + M_N^2 - M_S^2$.

The propagator for the $N^*(\frac{1}{2}^+)$-state reads:

$$\frac{\hat{P} + \sqrt{s}}{m^2 - s - G^2(s)\, B_{N^*}^{SN}(s)} \,, \tag{31}$$

with loop function $B_{N^*}^{SN}(s)$:

$$B_{N^*}^{SN}(s) = 2[(kP)B(s) + M_N^2 \tilde{B}(s)] \,. \tag{32}$$

The loop function $B(s)$ given in Eq. (11). The new basic term $\tilde{B}(s)$ reads as follows:

$$\tilde{B}(s) = \tilde{b}_0 + \frac{\sqrt{[s - (M_S + M_N)^2][s - (M_S - M_N)^2]}}{16\pi M_N \sqrt{s}} \tag{33}$$

$$\times \left[\frac{1}{\pi} \ln \frac{\sqrt{s[s - (M_S - M_N)^2]} - \sqrt{(M_N - M_S)^2[s - (M_S + M_N)^2]}}{\sqrt{s[s - (M_S - M_N)^2]} + \sqrt{(M_N - M_S)^2[s - (M_S + M_N)^2]}} + i \right] .$$

Singularities $s = 0$ and $s = (M_S - M_N)^2$ are absent in $\tilde{B}(s)$, the only present singularity is the threshold one $s = (M_S + M_N)^2$. In the determination of the $\tilde{B}(s)$ an uncertainty exists which is related to zeros of the loop functions; this item is discussed in Appendix A, subsection 7.3.

At $(M_S - M_N)^2 = 0$ the loop function has a simple form:

$$\tilde{B}(s) = \tilde{b}_0 + i\frac{\sqrt{[s - (M_S + M_N)^2]}}{16\pi M_N} \,. \tag{34}$$

4.2 Decay of the $N^*(\frac{1}{2}^+)$-state with the emission of a pseudoscalar meson

The propagator for the $N^*(\frac{1}{2}^+)$-state with the transition $N^*(\frac{1}{2}^+) \to \pi(0^-) + N(\frac{1}{2}^+) \to N^*(\frac{1}{2}^+)$ taken into account can be written as:

$$\frac{\hat{P} + \sqrt{s}}{m^2 - s - G^2(s)B_{N^*}^{\pi N}(s)} \,, \tag{35}$$

where $B_{N^*}^{\pi N}(s)$ is determined by the loop diagram $N^*(\frac{1}{2}^+) \to \pi(0^-) + N(\frac{1}{2}^+) \to N^*(\frac{1}{2}^+)$, namely:

$$B_{N^*}^{\pi N}(s) = \tag{36}$$

$$= \int \frac{d^4k}{i(2\pi)^4} \frac{i\hat{k}_{\perp}\gamma_5(\hat{k} + M_N)i\gamma_5\hat{k}_{\perp}}{(k^2 - M_N^2 - i0)((P-k)^2 - M_\pi^2 - i0)} \cdot (\hat{P} + \sqrt{s})$$

$$= \int \frac{d^4 k}{i(2\pi)^4} \frac{-k_\perp^2 (\frac{(kP)}{P^2}\hat{P} + M_N)}{(k^2 - M_N^2 - i0)((P-k)^2 - M_\pi^2 - i0)} \cdot (\hat{P} + \sqrt{s})$$

$$= \int \frac{d^4 k}{i(2\pi)^4} \frac{(\frac{(kP)^2}{P^2} - M_N^2)(\frac{(kP)}{P^2}\sqrt{s} + M_N)}{(k^2 - M_N^2 - i0)((P-k)^2 - M_\pi^2 - i0)} \cdot 2\sqrt{s} \,.$$

Recall, we use $k = k^\perp + \frac{(kP)}{P^2}P$ and $\hat{P} \to \sqrt{s}$.

The hadron rescattering factor is

$$B_{N^*}^{\pi N}(s) = 2(\frac{(kP)^2}{P^2} - M_N^2)\Big[(kP)B(s) + M_N^2\widetilde{B}(s)\Big]\,, \tag{37}$$

with $B(s)$ and $\widetilde{B}(s)$ given in Eqs. (11) and (33).

4.3   Transitions $\Delta(\frac{3}{2}^+) \to [N(\frac{1}{2}^+) + \pi(0^-)] \to \Delta(\frac{3}{2}^+)$

The propagator of the $\Delta(\frac{3}{2}^+)$-resonance, taking into account the transition $\Delta(\frac{3}{2}^+) \to N(\frac{1}{2}^+)\pi(0^-)$ (see Chapter 5 of ref. [27] and references therein) reads:

$$\frac{(-g_{\mu\nu}^\perp + \frac{1}{3}\gamma_\mu^\perp\gamma_\nu^\perp)(\hat{P} + \sqrt{s})}{m^2 - s - G^2(s)B_\Delta^{\pi N}(s)}\,, \tag{38}$$

see Appendix C for details. The factor $B_\Delta^{\pi N}(s)$ is determined by the P-wave loop diagram $\Delta(\frac{3}{2}^+) \to [N(\frac{1}{2}^+)\pi(0^-)]_{P-wave} \to \Delta(\frac{3}{2}^+)$, namely:

$$(-g_{\mu\nu}^\perp + \frac{1}{3}\gamma_\mu^\perp\gamma_\nu^\perp)(\hat{P} + \sqrt{s})\, B_\Delta^{\pi N}(s) \tag{39}$$

$$= (-g_{\mu\mu'}^\perp + \frac{1}{3}\gamma_\mu^\perp\gamma_{\mu'}^\perp)(\hat{P} + \sqrt{s}) \int \frac{d^4 k}{i(2\pi)^4} \frac{k_{\mu'}^\perp(\hat{k} + M_N)k_{\mu'}^\perp}{(k^2 - M_N^2 - i0)((P-k)^2 - M_\pi^2 - i0)}$$

$$\times (-g_{\nu'\nu}^\perp + \frac{1}{3}\gamma_{\nu'}^\perp\gamma_\nu^\perp)(\hat{P} + \sqrt{s})$$

$$= (g_{\mu\nu}^\perp - \frac{1}{3}\gamma_\mu^\perp\gamma_\nu^\perp)(\hat{P} + \sqrt{s}) \int \frac{d^4 k}{i(2\pi)^4} \frac{k_\perp^2 \left(\frac{(kP)}{P^2}\hat{P} + M_N\right)}{(k^2 - M_N^2 - i0)((P-k)^2 - M_\pi^2 - i0)} 2\sqrt{s}\,.$$

Therefore the πN rescattering factor can be written as ($k_\perp^2 = M_N^2 - \frac{(Pk)^2}{P^2}$):

$$B_\Delta^{\pi N}(s) = 2\Big(-M_N^2 + \frac{(Pk)^2}{s}\Big)\Big[(kP)B(s) + M_N^2\widetilde{B}(s)\Big]\,, \tag{40}$$

with $B(s)$ and $\widetilde{B}(s)$ given in eqs. (11) and (33).

5   Deuteron-like component

Let us consider in a more detailed way the case when the pole singularity is located near the threshold, $m \simeq M_a + M_b$. In this situation the deuteron-like component in the resonant state manifests itself evidently.

As an example we consider a case of the one-channel and one-pole amplitude, leading to S-wave decay-products. The scattering amplitude $ab \to ab$ reads:

$$\frac{1}{k}e^{i\delta}\sin\delta = \frac{G^2}{m^2 - s - G^2(B_\Re(s) + ik)} \tag{41}$$

where $B_\Re(s)$ is the real part of the loop diagram. Expanding this amplitude in a series over relative momentum of mesons, k, one has:

$$\frac{G^2}{[m^2 - (M_a + M_b)^2 - G^2 B_t] - k^2\frac{(M_a+M_b)^2}{M_a M_b}(1 + G^2 B_t') - ikG^2} \tag{42}$$
$$= \frac{a_0}{1 + \frac{1}{2}a_0 r_0 k^2 - ia_0 k} ,$$

here $B_t = B_\Re(s)_{s=(M_a+M_b)^2}$ and $B_t' = \left(\frac{dB_\Re(s)}{ds}\right)_{s=(M_a+M_b)^2}$, whereas a_0 is the scattering length and r_0 is the effective radius of the ab-system:

$$a_0 = \frac{G^2}{m^2 - (M_a + M_b)^2 - G^2 B_t} , \tag{43}$$
$$r_0 = -2\frac{(M_a + M_b)^2}{M_a M_b}(G^{-2} + B_t') .$$

At large negative a_0 the system has a stable component (an analog of the deuteron), at positive a_0 the resonance signal appears only in the continuous spectrum (the system is the analog of the singlet state in pp). A small value of $[m^2 - (M_a + M_b)^2 - G^2 B_t]$ (a large value of $|a_0|$) can exist independently of details of the long-range hadron-hadron interaction.

The large density of the levels in multi-particle systems enlarges the probability to face the effect of appearance of the deuteron-like components.

6 Conclusion

The hadron resonance topic is a key subject for both experimental studies and theoretical understanding in physics of elementary particles. An important point in this subject is the correct description of resonances. Using the language of hadron amplitudes this means a correct representation of the analytical structure of amplitudes. First of all, it concerns the propagators of resonances.

The experimental study of resonances is connected mainly to the investigation of multi-hadron reactions, the simplest reactions are three-particle ones. The description of Dalitz-plot data faces problems with the simultaneous presentation of resonances from different channels and the incorporation of requirements of the unitarity and analyticity into phenomenological analyses.

The use of three-body equations leads to implementing the analyticity and the three-body unitarity into the amplitude; in the non-relativistic case such an implementation can be performed using the Faddeev equation[21] while for the relativistic consideration the dispersion relation technique looks as the most appropriate one. In this case the resonance propagators

with included decay components are essential. But in the first attempts to write dispersion relation equations[22] problems appeared in choosing the way of integration.

A correct integration over a three-body intermediate state was performed in Ref. [23], the corresponding consequences of such an integration are discussed already for a long time.[24–26, 28] A realistic system of equations for coupled channel amplitudes for proton-antiproton annihilation at rest $[p\bar{p}]_{at\,rest} \to \pi\pi\pi,\ \eta\eta\pi,\ K\bar{K}\pi$ was written in Ref. [29] (see also Ref. [28], Chapter 5). A critical issue in the equations is the dispersion relation presentation of two-meson amplitudes and the corresponding resonances.

The multi-component structure of the constructed propagators for resonances allows to fix deuteron-like states. Examples are presented by states with hidden charm. There are several candidates for states with long-distant hadronic components: $X(3872) \to J/\Psi\pi\pi$ (nearby threshold $\bar{D}D^*$) [30] , $X(3900) \to J/\Psi\pi$ (nearby threshold $\bar{D}D^*$) [31], $X(4020) \to J/\Psi\pi$ (nearby threshold $\bar{D}^*D^*$) [32]. A popular interpretation of these states is that they are meson-meson molecules ($\bar{D}D^*$ and $\bar{D}^*D^*$). But it is possible that the states have two components, namely, short-range and long-range ones. That happens when a quark-gluon state (presumably a short-range one) is situated (may be accidentally) in the vicinity of the decay threshold.

To conclude: the construction of propagators of composite states with decay loop diagrams taken into account is a relevant subject for both experimental and theoretical studies in hadron physics.

Acknowledgement

Appendix A: Loop diagram analyticity

The convergence of the loop diagram, $B(s)$, can be guaranteed by introducing the vertex s-dependence or using the subtraction procedure:

$$\int\limits_{(M_a+M_b)^2}^{+\infty} \frac{ds'}{\pi} \frac{\rho_{\alpha'}(s')}{s'-s-i0} \to B(s=s_0) + \int\limits_{(M_a+M_b)^2}^{+\infty} \frac{ds'}{\pi} \frac{\rho_{\alpha'}(s')}{s'-s-i0} \cdot \frac{s-s_0}{s'-s_0}. \tag{44}$$

Here the subtraction procedure is used. In our studies we put $s_0 = (M_a + M_b)^2$.

We face two types of the imaginary parts for the loop diagrams:

$$Im\,B(s) = \frac{\sqrt{[s-(M_a+M_b)^2][s-(M_a-M_b)^2]}}{16\pi s}, \tag{45}$$

$$Im\,\widetilde{B}(s) = \frac{\sqrt{[s-(M_S+M_N)^2][s-(M_S-M_N)^2]}}{16\pi M_N \sqrt{s}}.$$

Within these imaginary parts we restore the loop diagrams, see Eqs. (11) and (33).

Meson-meson loop diagram

Let us consider the analytical sructure of the $B(s)$ in a more detailed way, keeping $s_0 = (M_a + M_b)^2$.

Below the threshold, at $(M_a - M_b)^2 < s < (M_a + M_b)^2$, the loop diagram reads:

$$
\begin{aligned}
B(s) &= b_0 + \beta \frac{(M_a + M_b)^2 - s}{s(M_a + M_b)^2} + i \frac{\sqrt{[-s + (M_a + M_b)^2][s - (M_a - M_b)^2]}}{16\pi s} \\
&\times \left[\frac{1}{\pi} \ln \frac{\sqrt{s - (M_a - M_b)^2} - i\sqrt{-s + (M_a + M_b)^2}}{\sqrt{s - (M_a - M_b)^2} + i\sqrt{-s + (M_a + M_b)^2}} + i \right] \\
&= b_0 + \beta \frac{(M_a + M_b)^2 - s}{s(M_a + M_b)^2} + i \frac{\sqrt{[-s + (M_a + M_b)^2][s - (M_a - M_b)^2]}}{16\pi s} \\
&\times \left[-\frac{2i}{\pi} \tan^{-1} \left(\frac{\sqrt{-s + (M_a + M_b)^2}}{\sqrt{s - (M_a - M_b)^2}} \right) + i \right].
\end{aligned}
\tag{46}
$$

The last line demonstrates the absence of a singularity in $s = (M_a - M_b)^2$. Indeed, in the top-down approach to this point we have:

$$
\begin{aligned}
&-\frac{2i}{\pi} \tan^{-1} \left(\frac{\sqrt{-s + (M_a + M_b)^2}}{\sqrt{s - (M_a - M_b)^2}} \right) + i \\
&= -\frac{2i}{\pi} \left(\frac{\pi}{2} - \tan^{-1} \frac{\sqrt{s - (M_a - M_b)^2}}{\sqrt{-s + (M_a + M_b)^2}} \right) + i \\
&\simeq -\frac{2i}{\pi} \left(\frac{\pi}{2} - \frac{\sqrt{s - (M_a - M_b)^2}}{\sqrt{-s + (M_a + M_b)^2}} \right) + i
\end{aligned}
\tag{47}
$$

with the corresponding cancellation of the singular terms in Eq. (48).

Meson-baryon loop diagram

The meson-nucleon loop diagram $\widetilde{B}(s)$ below the threshold, at $(M_S - M_N)^2 < s < (M_S + M_N)^2$, reads:

$$
\begin{aligned}
\widetilde{B}(s) &= \widetilde{b}_0 + i \frac{\sqrt{[-s + (M_S + M_N)^2][s - (M_S - M_N)^2]}}{16\pi M_N \sqrt{s}} \\
&\times \left[\frac{1}{\pi} \ln \frac{\sqrt{s[s - (M_S - M_N)^2]} - i|M_N - M_S|\sqrt{-s + (M_S + M_N)^2}}{\sqrt{s[s - (M_S - M_N)^2]} + i|M_N - M_S|\sqrt{-s + (M_S + M_N)^2}} + i \right] \\
&= \widetilde{b}_0 + i \frac{\sqrt{[-s + (M_S + M_N)^2][s - (M_S - M_N)^2]}}{16\pi M_N \sqrt{s}} \\
&\times \left[-\frac{2i}{\pi} \tan^{-1} \left(\frac{|M_N - M_S|\sqrt{-s + (M_S + M_N)^2}}{\sqrt{s[s - (M_S - M_N)^2]}} \right) + i \right].
\end{aligned}
\tag{48}
$$

Near $s = (M_S - M_N)^2$ we write:

$$\tan^{-1} \left(\frac{|M_N - M_S|\sqrt{-s + (M_S + M_N)^2}}{\sqrt{s[s - (M_S - M_N)^2]}} \right)$$

$$= \frac{\pi}{2} - \tan^{-1} \frac{\sqrt{s[s - (M_S - M_N)^2]}}{|M_N - M_S|\sqrt{-s + (M_S + M_N)^2}} \right) \tag{49}$$

and the meson-nucleon loop diagram $\widetilde{B}(s)$ below the threshold is:

$$\widetilde{B}(s) = \widetilde{b}_0 + \frac{\sqrt{[-s + (M_S + M_N)^2][s - (M_S - M_N)^2]}}{16\pi M_N \sqrt{s}}$$

$$\times \left[-\frac{2}{\pi} \tan^{-1} \frac{\sqrt{s[s - (M_S - M_N)^2]}}{|M_N - M_S|\sqrt{-s + (M_S + M_N)^2}} \right]. \tag{50}$$

It is seen that points $s = 0$ and $s = (M_S - M_N)^2$ are non-singular. Moreover, at $s = (M_S - M_N)^2$ we have $\widetilde{B}(s) = \widetilde{b}_0$, see Eq. (50), that corresponds to zero of the s-dependent part of the loop diagram. Ambiguities in the determimation of the loop diagrams are related to zeros of $B(s)$ and $\widetilde{B}(s)$.

Ambiguites in the determination of the resonance amplitude

The ambiguities of the resonance amplitude are due to CDD-poles [20] . The resonance amplitude with CDD-poles taken into account is written as follows:

$$\frac{B(s)}{1 - B(s) + \sum_n \frac{\gamma_n}{s - s_n}} \tag{51}$$

A redefinition of the type

$$B(s) \rightarrow \frac{B(s)}{1 + \sum_n \frac{\gamma_n}{s - s_n}} \tag{52}$$

returns us to the used form of amplitudes. But the redefined $B(s)$ differs in numbers and the positions of zeros.

Appendix B: Angular momentum operators for two-meson systems

We use angular momentum operators $X^{(L)}_{\mu_1 \dots \mu_L}(k^\perp)$, $Z^\alpha_{\mu_1 \dots \mu_L}(k^\perp)$ and the projection operator $O^{\mu_1 \dots \mu_L}_{\nu_1 \dots \nu_L}(\perp P)$ (see [27, 28, 33]). Let us recall their definition.

The operators are constructed from the relative momenta $k^\perp_\mu$ and tensor $g^\perp_{\mu\nu}$. Both of them are orthogonal to the total momentum of the system:

$$k^\perp_\mu = \frac{1}{2} g^\perp_{\mu\nu}(k_1 - k_2)_\nu = k_{1\nu} g^{\perp P}_{\nu\mu} = -k_{2\nu} g^{\perp P}_{\nu\mu}, \qquad g^\perp_{\mu\nu} = g_{\mu\nu} - \frac{P_\mu P_\nu}{s} . \tag{53}$$

The operator for $L = 0$ is a scalar (we write $X^{(0)}(k^\perp) = 1$), and the operator for $L = 1$ is a vector, $X^{(1)}_\mu = k^\perp_\mu$. The operators $X^{(L)}_{\mu_1\ldots\mu_L}$ for $L \geq 1$ can be written in the form of a recurrency relation:

$$
\begin{aligned}
X^{(L)}_{\mu_1\ldots\mu_L}(k^\perp) &= k^\perp_\alpha Z^\alpha_{\mu_1\ldots\mu_L}(k^\perp) \equiv k^\perp_\alpha Z_{\mu_1\ldots\mu_L,\alpha}(k^\perp), \\
Z^\alpha_{\mu_1\ldots\mu_L}(k^\perp) &\equiv Z_{\mu_1\ldots\mu_L,\alpha}(k^\perp) = \frac{2L-1}{L^2}\Big(\sum_{i=1}^{L} X^{(L-1)}_{\mu_1\ldots\mu_{i-1}\mu_{i+1}\ldots\mu_L}(k^\perp)g^\perp_{\mu_i\alpha} - \\
&\quad -\frac{2}{2L-1}\sum_{\substack{i,j=1\\i<j}}^{L} g^\perp_{\mu_i\mu_j}\, X^{(L-1)}_{\mu_1\ldots\mu_{i-1}\mu_{i+1}\ldots\mu_{j-1}\mu_{j+1}\ldots\mu_L\alpha}(k^\perp)\Big).
\end{aligned}
\tag{54}
$$

We have a convolution equality $X^{(L)}_{\mu_1\ldots\mu_L}(k^\perp)k^\perp_{\mu_L} = k^2_\perp X^{(L-1)}_{\mu_1\ldots\mu_{L-1}}(k^\perp)$, with $k^2_\perp \equiv k^\perp_\mu k^\perp_\mu$, and the tracelessness property of $X^{(L)}_{\mu\mu\mu_3\ldots\mu_L} = 0$. On this basis, one can write down the normalization condition for orbital angular operators:

$$
\int \frac{d\Omega}{4\pi} X^{(L)}_{\mu_1\ldots\mu_L}(k^\perp)X^{(L)}_{\mu_1\ldots\mu_L}(k^\perp) = \alpha_L k^{2L}_\perp, \quad \alpha_L = \prod_{l=1}^{L}\frac{2l-1}{l},
\tag{55}
$$

where the integration is performed over spherical variables $\int d\Omega/(4\pi) = 1$.

Iterating Eq. (54), one obtains the following expression for the operator $X^{(L)}_{\mu_1\ldots\mu_L}$ at $L \geq 1$:

$$
\begin{aligned}
X^{(L)}_{\mu_1\ldots\mu_L}(k^\perp) = \alpha_L \Big[& k^\perp_{\mu_1}k^\perp_{\mu_2}k^\perp_{\mu_3}k^\perp_{\mu_4}\ldots k^\perp_{\mu_L} - \\
&-\frac{k^2_\perp}{2L-1}\Big(g^\perp_{\mu_1\mu_2}k^\perp_{\mu_3}k^\perp_{\mu_4}\ldots k^\perp_{\mu_L} + g^\perp_{\mu_1\mu_3}k^\perp_{\mu_2}k^\perp_{\mu_4}\ldots k^\perp_{\mu_L} + \ldots\Big) + \\
&+\frac{k^4_\perp}{(2L-1)(2L-3)}\Big(g^\perp_{\mu_1\mu_2}g^\perp_{\mu_3\mu_4}k^\perp_{\mu_5}k^\perp_{\mu_6}\ldots k^\perp_{\mu_L} \\
&+ g^\perp_{\mu_1\mu_2}g^\perp_{\mu_3\mu_5}k^\perp_{\mu_4}k^\perp_{\mu_6}\ldots k^\perp_{\mu_L} + \ldots\Big) + \ldots\Big].
\end{aligned}
\tag{56}
$$

For the projection operators, one has:

$$
\begin{aligned}
O &= 1, \qquad O^\mu_\nu(\perp P) = g^\perp_{\mu\nu}, \\
O^{\mu_1\mu_2}_{\nu_1\nu_2}(\perp P) &= \frac{1}{2}\Big(g^\perp_{\mu_1\nu_1}g^\perp_{\mu_2\nu_2} + g^\perp_{\mu_1\nu_2}g^\perp_{\mu_2\nu_1} - \frac{2}{3}g^\perp_{\mu_1\mu_2}g^\perp_{\nu_1\nu_2}\Big).
\end{aligned}
\tag{57}
$$

For higher states, the operator can be calculated using the recurrent expression:

$$
\begin{aligned}
O^{\mu_1\ldots\mu_L}_{\nu_1\ldots\nu_L}(\perp P) = \frac{1}{L^2}\Big(& \sum_{i,j=1}^{L} g^\perp_{\mu_i\nu_j} O^{\mu_1\ldots\mu_{i-1}\mu_{i+1}\ldots\mu_L}_{\nu_1\ldots\nu_{j-1}\nu_{j+1}\ldots\nu_L}(\perp P) - \\
&-\frac{4}{(2L-1)(2L-3)}\times\sum_{\substack{i<j\\k<m}}^{L} g^\perp_{\mu_i\mu_j}g^\perp_{\nu_k\nu_m} O^{\mu_1\ldots\mu_{i-1}\mu_{i+1}\ldots\mu_{j-1}\mu_{j+1}\ldots\mu_L}_{\nu_1\ldots\nu_{k-1}\nu_{k+1}\ldots\nu_{m-1}\nu_{m+1}\ldots\nu_L}(\perp P)\Big).
\end{aligned}
\tag{58}
$$

The projection operators obey the relations:

$$
\begin{aligned}
O^{\mu_1\ldots\mu_L}_{\nu_1\ldots\nu_L}(\perp P)X^{(L)}_{\nu_1\ldots\nu_L}(k^\perp) &= X^{(L)}_{\mu_1\ldots\mu_L}(k^\perp), \\
O^{\mu_1\ldots\mu_L}_{\nu_1\ldots\nu_L}(\perp P)k_{\nu_1}k_{\nu_2}\ldots k_{\nu_L} &= \frac{1}{\alpha_L}X^{(L)}_{\mu_1\ldots\mu_L}(k^\perp).
\end{aligned}
\tag{59}
$$

15

Hence, the product of the two $X^L(k_\perp)$ operators results in the Legendre polynomials as follows:

$$X^{(L)}_{\mu_1...\mu_L}(k_1^\perp)(-1)^L O^{\mu_1...\mu_L}_{\nu_1...\nu_L}(\perp P)X^{(L)}_{\nu_1...\nu_L}(k_2^\perp)=\alpha_L\left(\sqrt{-k_1^{\perp 2}}\sqrt{-k_2^{\perp 2}}\right)^L P_L(z), \qquad (60)$$

where $z \equiv (-k_{1\nu}^\perp k_{2\nu}^\perp)/(\sqrt{-k_1^{\perp 2}}\sqrt{-k_2^{\perp 2}})$.

Appendix C: Baryon resonances, wave functions and propagators

We construct spin-dependent propagators which do not change their spin structure with the inclusion of the loop-diagram interaction. The corresponding spin wave functions are eigenfunctions for the interaction. In the framework of this procedure we work with the effective mass of the system, and this effective mass depends on the energy, $M(s)$. For resonance systems we write $M^2(s) = s$, for detail see [27, 28, 34, 35].

Baryon spin-1/2 wave function

The spin-dependent numerator of the D-function reads:

$$\sum_{j=1,2} \psi_j(p)\,\bar\psi_j(p) = \hat{p} + M(s), \qquad \sum_{j=3,4} \psi_j(p)\,\bar\psi_j(p) = -(\hat{p} + M(s)) . \qquad (61)$$

where $M(s)$ is the effective mass of the resonance system. It means that we work with baryon wave functions $\psi(p)$ and $\bar\psi(p) = \psi^+(p)\gamma_0$ which obey the following equations for spin-1/2 fermions:

$$(\hat{p} - M(s))\psi(p) = 0, \qquad \bar\psi(p)(\hat{p} - M(s)) = 0, \qquad (62)$$

Wave functions are normalised as follows:

$$j, j' = 1, 2 \;\; : \;\; \left(\bar\psi_j(p)\psi_{j'}(p)\right) = 2M(s)\,\delta_{jj'},$$
$$j, j' = 3, 4 \;\; : \;\; \left(\bar\psi_j(p)\psi_{j'}(p)\right) = -2M(s)\,\delta_{jj'}. \qquad (63)$$

The solution of the equation (62) gives us four wave functions:

$$j = 1, 2 \;\; : \;\; \psi_j(p) = \sqrt{p_0 + M(s)}\left(\begin{array}{c} \varphi_j \\ \frac{(\boldsymbol{\sigma p})}{p_0+M(s)}\,\varphi_j \end{array}\right),$$

$$\bar\psi_j(p) = \sqrt{p_0 + M(s)}\left(\varphi_j^+, -\varphi_j^+\frac{(\boldsymbol{\sigma p})}{p_0 + M(s)}\right) ,$$

$$j = 3, 4 \;\; : \;\; \psi_j(-p) = i\sqrt{p_0 + M(s)}\left(\begin{array}{c} \frac{(\boldsymbol{\sigma p})}{p_0+M(s)}\,\chi_j \\ \chi_j \end{array}\right),$$

$$\bar\psi_j(-p) = -i\sqrt{p_0 + M(s)}\left(\chi_j^+\frac{(\boldsymbol{\sigma p})}{p_0 + M(s)}, -\chi_j^+\right), \qquad (64)$$

where φ_j and χ_j are two-component spinors normalised as $\varphi_j^+\varphi_{j'} = \delta_{jj'}$ and $\chi_j^+\chi_{j'} = \delta_{jj'}$.

Solutions with $j = 3, 4$ refer to antibaryons. The corresponding wave function is defined as

$$j = 3, 4: \quad \psi_j^c(p) = C\bar{\psi}_j^T(-p), \quad C^{-1}\gamma_\mu C = -\gamma_\mu^T. \tag{65}$$

We see that $\psi_j^c(p)$ satisfies the equation:

$$(\hat{p} - M(s))\psi_j^c(p) = 0. \tag{66}$$

Spin-$\frac{3}{2}$ wave functions

To describe resonance states Δ and $\bar{\Delta}$, we use the wave functions $\psi_\mu(p)$ and $\bar{\psi}_\mu(p) = \psi_\mu^+(p)\gamma_0$ which satisfy the following constraints:

$$(\hat{p} - M(s))\psi_\mu(p) = 0, \qquad \bar{\psi}_\mu(p)(\hat{p} - M(s)) = 0,$$
$$p_\mu\psi_\mu(p) = 0, \qquad \gamma_\mu\psi_\mu(p) = 0. \tag{67}$$

Here $\psi_\mu(p)$ is a four-component spinor and μ is a four-vector index. Sometimes, to underline spin variables, we use the notation $\psi_\mu(p; j)$.

Wave function for Δ

The equation (67) gives four wave functions for the Δ:

$$j = 1, 2: \quad \psi_\mu(p; j) = \sqrt{p_0 + M(s)} \begin{pmatrix} \varphi_{\mu\perp}(j) \\ \frac{(\boldsymbol{\sigma p})}{p_0 + M(s)} \varphi_{\mu\perp}(j) \end{pmatrix},$$

$$\bar{\psi}_\mu(p; j) = \sqrt{p_0 + M(s)} \left(\varphi_{\mu\perp}^+(j), -\varphi_{\mu\perp}^+(j)\frac{(\boldsymbol{\sigma p})}{p_0 + M(s)} \right), \tag{68}$$

where the two-component spinors $\varphi_{\mu\perp}(a)$ are determined to be perpendicular to p_μ thus keeping for Δ four independent spin components $\mu_z = 3/2, 1/2, -1/2, -3/2$ related to the spin $S = 3/2$ and removing the components with $S = 1/2$.

The completeness conditions for the spin-$\frac{3}{2}$ wave functions can be written as follows:

$$\sum_{j=1,2} \psi_\mu(p; j)\, \bar{\psi}_\nu(p; j) = (\hat{p} + M(s))\left(-g_{\mu\nu}^\perp + \frac{1}{3}\gamma_\mu^\perp\gamma_\nu^\perp \right)$$

$$= (\hat{p} + M(s))\frac{2}{3}\left(-g_{\mu\nu}^\perp + \frac{1}{2}\sigma_{\mu\nu}^\perp \right), \tag{69}$$

where $g_{\mu\nu}^\perp \equiv g_{\mu\nu}^{\perp p}$ and $\gamma_\mu^\perp = g_{\mu\mu'}^{\perp p}\gamma_{\mu'}$. The factor $(\hat{p} + M(s))$ commutates with $(g_{\mu\nu}^\perp - \frac{1}{3}\gamma_\mu^\perp\gamma_\nu^\perp)$ in (69) because $\hat{p}\gamma_\mu^\perp\gamma_\nu^\perp = \gamma_\mu^\perp\gamma_\nu^\perp\hat{p}$. The matrix $\sigma_{\mu\nu}^\perp$ is determined in a standard way, $\sigma_{\mu\nu}^\perp = \frac{1}{2}(\gamma_\mu^\perp\gamma_\nu^\perp - \gamma_\nu^\perp\gamma_\mu^\perp)$.

Wave function for $\bar{\Delta}$

The anti-delta, $\bar{\Delta}$, is determined by the following four wave functions:

$$j = 3, 4: \quad \psi_\mu(-p; j) = i\sqrt{p_0 + M(s)} \begin{pmatrix} \frac{(\boldsymbol{\sigma p})}{p_0 + M(s)} \chi_{\mu\perp}(j) \\ \chi_{\mu\perp}(j) \end{pmatrix},$$

$$\bar{\psi}_\mu(-p; j) = -i\sqrt{p_0 + M(s)} \left(\chi_{\mu\perp}^+(j)\frac{(\boldsymbol{\sigma p})}{p_0 + M(s)}, -\chi_{\mu\perp}^+(j) \right). \tag{70}$$

The completeness conditions for spin-$\frac{3}{2}$ wave functions with $j = 3, 4$ are

$$
\sum_{j=3,4} \psi_\mu(-p;j)\,\bar{\psi}_\nu(-p;j) = -(\hat{p}+M(s))\left(-g_{\mu\nu}^\perp + \frac{1}{3}\gamma_\mu^\perp\gamma_\nu^\perp\right)
$$

$$
= -(\hat{p}+M(s))\frac{2}{3}\left(-g_{\mu\nu}^\perp + \frac{1}{2}\sigma_{\mu\nu}^\perp\right). \tag{71}
$$

The equation (70) can be rewritten in the form of (68) using the charge conjugation matrix C which was introduced for spin-$\frac{1}{2}$ particles. We write:

$$
j = 3, 4 \quad : \quad \psi_\mu^c(p;j) = C\bar{\psi}_\mu^T(-p;j). \tag{72}
$$

The wave functions $\psi_\mu^c(p;j)$ with $j = 3, 4$ obey the equation:

$$
(\hat{p}-M(s))\,\psi_\mu^c(p;j) = 0 \ . \tag{73}
$$

Projection operators for resonance states with $J > 3/2$.

The wave function of a resonance state with spin $J = \ell + 1/2$, momentum p and effective mass term $M(s)$ is given by a tensor four-spinor $\psi_{\mu_1...\mu_\ell}$. It satisfies the constraints

$$
(\hat{p}-M(s))\psi_{\mu_1...\mu_\ell} = 0, \quad p_{\mu_i}\psi_{\mu_1...\mu_\ell} = 0, \quad \gamma_{\mu_i}\psi_{\mu_1...\mu_\ell} = 0, \tag{74}
$$

and the symmetry properties

$$
\psi_{\mu_1...\mu_i...\mu_j...\mu_\ell} = \psi_{\mu_1...\mu_j...\mu_i...\mu_\ell}\ ,
$$

$$
g_{\mu_i\mu_j}\psi_{\mu_1...\mu_i...\mu_j...\mu_\ell} = g_{\mu_i\mu_j}^{\perp p}\psi_{\mu_1...\mu_i...\mu_j...\mu_\ell} = 0. \tag{75}
$$

Conditions (74), (75) define the structure of the denominator of the fermion propagator (the projection operator) which can be written in the following form:

$$
F_{\nu_1...\nu_\ell}^{\mu_1...\mu_\ell}(p) = (-1)^\ell(\hat{p}+M(s))\Phi_{\nu_1...\nu_\ell}^{\mu_1...\mu_\ell}(\perp p). \tag{76}
$$

The operator $\Phi_{\nu_1...\nu_\ell}^{\mu_1...\mu_\ell}(\perp p)$ describes the tensor structure of the propagator. It is equal to 1 for a ($J = 1/2$)-particle and is proportional to $g_{\mu\nu}^{\perp p} - \gamma_\mu^\perp\gamma_\nu^\perp/3$ for a particle with spin $J = 3/2$ (remind that $\gamma_\mu^\perp = g_{\mu\nu}^{\perp p}\gamma_\nu$).

The conditions (5)-(9) are identical for fermion and boson projection operators and therefore the fermion projection operator can be written as:

$$
\Phi_{\nu_1...\nu_\ell}^{\mu_1...\mu_\ell}(\perp p) = O_{\alpha_1...\alpha_\ell}^{\mu_1...\mu_\ell}(\perp p)\phi_{\beta_1...\beta_\ell}^{\alpha_1...\alpha_\ell}(\perp p)O_{\nu_1...\nu_\ell}^{\beta_1...\beta_\ell}(\perp p)\ . \tag{77}
$$

The operator $\phi_{\beta_1...\beta_\ell}^{\alpha_1...\alpha_\ell}(\perp p)$ can be expressed in a rather simple form since all symmetry and orthogonality conditions are imposed by O-operators. First, the ϕ-operator is constructed of metric tensors only, which act in the space of $\perp p$ and $\gamma^\perp$-matrices. Second, a construction like $\gamma_{\alpha_i}^\perp\gamma_{\alpha_j}^\perp = \frac{1}{2}g_{\alpha_i\alpha_j}^\perp + \sigma_{\alpha_i\alpha_j}^\perp$ (remind that here $\sigma_{\alpha_i\alpha_j}^\perp = \frac{1}{2}(\gamma_{\alpha_i}^\perp\gamma_{\alpha_j}^\perp - \gamma_{\alpha_j}^\perp\gamma_{\alpha_i}^\perp)$) gives zero if multiplied by an $O_{\alpha_1...\alpha_\ell}^{\mu_1...\mu_\ell}$-operator: the first term is due to the traceless conditions and the second one to symmetry properties. The only structures which can then be constructed are $g_{\alpha_i\beta_j}^\perp$ and $\sigma_{\alpha_i\beta_j}^\perp$.

Moreover, taking into account the symmetry properties of the O-operators, one can use any pair of indices from sets $\alpha_1 \ldots \alpha_\ell$ and $\beta_1 \ldots \beta_\ell$, for example, $\alpha_i \to \alpha_1$ and $\beta_j \to \beta_1$. Then

$$\phi^{\alpha_1 \ldots \alpha_\ell}_{\beta_1 \ldots \beta_\ell}(\perp p) = \frac{\ell+1}{2\ell+1}(g^{\perp}_{\alpha_1\beta_1} - \frac{\ell}{\ell+1}\sigma^{\perp}_{\alpha_1\beta_1})\prod_{i=2}^{\ell} g^{\perp}_{\alpha_i\beta_i}. \tag{78}$$

Since $\Phi^{\mu_1 \ldots \mu_\ell}_{\nu_1 \ldots \nu_\ell}(\perp p)$ is determined by convolutions of O-operators, see Eq. (77), we can replace in (77)

$$\phi^{\alpha_1 \ldots \alpha_\ell}_{\beta_1 \ldots \beta_\ell}(\perp p) \to \phi^{\alpha_1 \ldots \alpha_\ell}_{\beta_1 \ldots \beta_\ell}(p) = \frac{\ell+1}{2\ell+1}(g_{\alpha_1\beta_1} - \frac{\ell}{\ell+1}\sigma_{\alpha_1\beta_1})\prod_{i=2}^{\ell} g_{\alpha_i\beta_i}. \tag{79}$$

The coefficients in (79) are chosen to satisfy the constraints (74) and the convolution condition:

$$\Phi^{\mu_1 \ldots \mu_\ell}_{\alpha_1 \ldots \alpha_\ell}(p)\Phi^{\alpha_1 \ldots \alpha_\ell}_{\nu_1 \ldots \nu_\ell}(p) = \Phi^{\mu_1 \ldots \mu_\ell}_{\nu_1 \ldots \nu_\ell}(p) . \tag{80}$$

References

[1] S. Amato et al., *Summary of the 2015 LHCb workshop on multi-body decays of D and B mesons,* arXiv:1605.03889 [hep-ex].

[2] LHCb, R. Aaij et al., Phys. Rev. Lett. **115** 072001 (2015).

[3] M. Karliner, T. Skwarnicki, *Pentaquarks,* PDG (2016).

[4] M.B. Voloshin, L.B. Okun, JETP Letters, **53** (1976) 333, [Pisma ZETF 23 , 369 (1976)].

[5] A. De Rujula, H. Greorgi, S.L. Glashow, Phys.Rev.Lett. **38** (1977) 317.

[6] Y. Shimizu, D. Suenaga, M. Harada, *Coupled channel analysis of molecule picture of $P_c(4380)$,* arXiv:1603.02376 [hep-ph].

[7] X.-H. Liu, M. Oka, *Understanding the nature of the heavy quarks and searching for them in pion induced reactions,* arXiv:1602.07069 [hep-ph].

[8] L. Roca, E. Oset, *On the hidden charm pentaquarks in $\Lambda \to J/\psi K^- p$ decay,* arXiv:1602.06791 [hep-ph].

[9] H.-X. Chen, W. Chen, X. Liu, S.-L. Zhu, *The hidden charm pentaquark and tetraquark states,* arXiv:1601.02092 [hep-ph].

[10] H.-X. Chen, R.-L. Cui, W. Chen, T.G. Steele, X. Liu, S.-L. Zhu, *QCD sum rule study of hidden-charm pentaquarks,* arXiv:1601.02092 [hep-ph].

[11] R.F. Lebed, Phys.Rev. D**92** (2015) 114030.

[12] S. Stone, *Exotic hadrons in hadron collisions,* PoS FPCP2015(2015)041; *Pentaquarks and tetraquarks at LHCb,* PoS FPCP2015(2015)434.

[13] X.-Y. Cheng, C.K. Chua, Phys. Rev. D**92** (2015) 086009.

[14] T.J. Burns, Eur.Phys.J. A51 (2015) 152.

[15] L. Maiani, A.D. Polosa, V. Riquer, Phys. Lett. **B750** (2015) 37.

[16] V.V. Anisovich, M.A. Matveev, J. Nyiri, A.V. Sarantsev, A.N. Semenova, *Pentaquarks and resonances in the pJ/ψ spectrum*, arXiv:1507.07652 [hep-ph].

[17] V.V. Anisovich, M.A. Matveev, A.V. Sarantsev, and A.N. Semenova, Int. J. Mod. Phys. **A30**, no. 32, (2015) 1550186.

[18] G. Breit and E. Wigner, Phys. Rev. **36**, 519 (1936).

[19] M. Gell-Mann and K.M. Watson, Ann. Rev. Nucl. Sci., Standford (1954).

[20] L. Castllejo, R.H. Dalitz, F.J. Dyson, Phys. Rev. **101**, 453 (1956).

[21] L.D. Faddeev, ZhETP **39**,1459 (1960), [Sov. Phys. JETP **12**, 1014 (1961)].

[22] N.N. Khuri, S.B. Treiman, Phys. Rev. **119**, 1115 (1960).

[23] V.V. Anisovich, A.A. Anselm, V.N. Gribov, *On the theory of reactions with the productions of three low-energy particles*, Nucl. Phys. **38**, 132 (1962).

[24] I.J.R. Aitchison, S. Pasquier, Phys. Rev. **152**, 1276 (1966).

[25] V.V. Anisovich, L.G. Dakhno, Nucl. Phys. **76**, 657 (1966).

[26] I.J.R. Aitchison, *Unitarity, analytisity and crossing symmetry in two- and three-hadron final state interactions*, arXiv:1507.02697 [hep-ph].

[27] A.V. Anisovich, V.V. Anisovich, M.A. Matveev, V.A. Nikonov, J. Nyiri, A.V. Sarantsev, *Mesons and baryons. Systematization and methods of analisis.*, World Scientific Publishing (2008).

[28] A.V. Anisovich, V.V. Anisovich, M.A. Matveev, V.A. Nikonov, J. Nyiri, A.V. Sarantsev, *Three-particle physics and dispersion relation theory*, World Scientific Publishing (2013).

[29] A.V. Anisovich, Yad. Fiz. **66**, 173 (2003); [Phys. Atom. Nucl. **66** 172 (2003)].

[30] BESIII, Phys. Rev. Lett. **110** (2013) 252001.

[31] T. Xiao et al., Phys. Lett. **B727** (2013) 366.

[32] BESIII, M. Ablikim et al., Phys. Rev. Lett. **113** (2014) no. 21 212002; Phys. Rev. Lett. **111** (2013) no. 24 242001.

[33] A.V. Anisovich, V.V. Anisovich, V.N. Markov, M.A. Matveev, A.V. Sarantsev, *Moment operator expansion for the two meson, two photon and fermion anti-fermion states*, J. Phys. G**28** (2002) 15-32, hep-ph/0105330.

[34] A.V. Anisovich, *Partial wave analysis of the two neutral pion photoproduction data*, AIP Conf. Proc. **717** 250 (2004).

[35] A.V. Anisovich, A.V. Sarantsev *Partial decay widths of baryons in the spin-momentum operator expansion method*, Eur.Phys.J. A30 (2006) 427-441, hep-ph/0605135.